Charles University in Prague
First Faculty of Medicine

PhD thesis summary

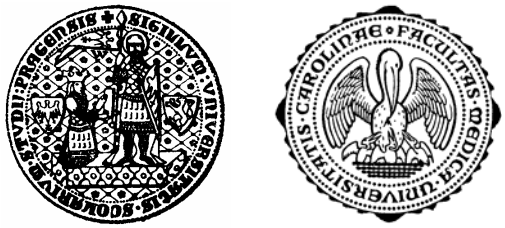

Biochemical and molecular studies of cytochrome c oxidase and ATP synthase deficiencies

Mgr. Daniela Fornůsková

2010

Doktorské studijní programy v biomedicíně

Univerzita Karlova v Praze a Akademie věd České republiky

Obor:	biochemie a patobiochemie
Předseda oborové rady:	Prof. MUDr. Jiří Kraml, DrSc.
Školící pracoviště:	Laboratoř pro studium mitochondriálních poruch Klinika dětského a dorostového lékařství 1. lékařská fakulta, Univerzita Karlova v Praze Ke Karlovu 2, 128 08 Praha 2
Školitel:	Prof. MUDr. Jiří Zeman, DrSc.

Disertační práce bude nejméně pět pracovních dnů před konáním obhajoby zveřejněna k nahlížení veřejnosti v tištěné podobě na Oddělení pro vědeckou činnost a zahraniční styky Děkanátu 1. lékařské fakulty.

Postgraduate studies in Biomedicine

Charles University in Prague and Academy of Sciences of the Czech Republic

Section:	biochemistry and pothobiochemistry
Section chairman:	Prof. MUDr. Jiří Kraml, DrSc.
Supervising department:	Laboratory for study of mitochondrial disorders Department of Pediatrics and Adolescent Medicine First Faculty of Medicine, Charles University in Prague Ke Karlovu 2, 128 08 Prague 2
Supervisor:	Prof. MUDr. Jiří Zeman, DrSc.

The PhD thesis was elaborated during Postgraduate Studies in Biomedicine at the First Faculty of Medicine of Charles University in Prague within years 2004 – 2010 and was supported by grants from the Grant Agency of Charles University [grant number GAUK 153/2004/C] and [grant number GAUK 1/2006/R], the Grant Agency of Czech Republic [grant number GACR 303/03/H065], the Internal Grant Agency of the Ministry of Health of the Czech Republic [grant number IGA MZ NS 10581/3] and by institutional project [grant number MSM 0021620806].

LIST OF CONTENTS

ABBREVIATIONS

2D	two-dimensional
Δ	deletion
ΔΨ	potential difference
$\Delta\Psi_m$	mitochondrial membrane potential
ΔpH	proton gradient
ADP	adenosine diphosphate
AMP	adenosine monophosphate
ATP	adenosine triphosphate
ATPase	adenosine triphosphatase
BN	blue native
bp	base pair
BSA	bovine serum albumin
CcO	cytochrome c oxidase, complex IV
CI	complex I
CII	complex II
CIII	complex III
CIV	complex IV
CMV	cytomegalovirus (RNA polymerase II) promoter
CN	colorless native
CNS	central nervous system
CoQ	coenzyme Q
COX	cytochrome c oxidase, complex IV
Cox#	cytochrome c oxidase structural subunit number #
CS	citrate synthase
CV	complex V
CytC	cytochrome c
dCTP	deoxy-cytosine triphosphate
DDM	n-dodecyl-β-D-maltoside
DMSO	dimethyl sulfoxide
DNA	deoxyribonucleic acid
EDTA	ethylenediaminetetraacetic acid
EGTA	ethylene glycol tetraacetic acid
FACS	fluorescent-activated cell sorting
FAD	flavin adenine dinucleotide
$FADH_2$	flavin adenine dinucleotide reduced
FCCP	carbonyl cyanide *p*-trifluoromethoxyphenylhydrazone
FLAG	octapeptide tag sequence (N-DYKDDDDK-C, 1012 Da)
GFP	green fluorescent protein
HEK-293	human embryonic kidney - 293
IMAGE	integrated molecular analysis of genomes and their expression
IMM	inner mitochondrial membrane
IMS	intermembrane space
IRES-Neo	internal ribosome entry site - neomycin phosphotransferase
KD	knockdown

kDa	kilodalton
MDa	megadalton
MELAS	mitochondrial encephalopathy, lactic acidosis, and stroke like episodes
MERRF	myoclonic epilepsy and ragged-red fibers
mRNA	messenger ribonucleic acid
mt	mitochondrial
mt-tRNA	mitochondrial transfer ribonucleic acid
MW	molecular weight
n	nuclear
NAD^+	nicotinamide adenine dinucleotide
NADH	nicotinamide adenine dinucleotide reduced
NS	non-silencing
nt	nucleotide(s)
ORF	open reading frame
OXA1	oxidase assembly 1
OXA1L	oxidase assembly 1-like
OXPHOS	oxidative phosphorylation system
P_{50}	partial pressure of oxygen at half-maximal respiration rate
PAGE	polyacrylamide gel electrophoresis
PBS	phosphate-buffered saline
PCR	polymerase chain reaction
Pi	inorganic phosphate
PMF	proton motive force
PVDF	polyvinylidene difluoride
QCR	ubiquinol:cytochrome *c* oxidoreductase, complex III
qRT-PCR	quantitative real-time PCR
RFLP	restriction fragment length polymorphism
RNA	ribonucleic acid
RNAi	RNA interference
ROS	reactive oxygen species
rRNA	ribosomal ribonucleic acid
SDH	succinate dehydrogenase
SDS	sodium dodecyl sulfate
shRNA	short hairpin RNA
shRNAmir	microRNA-adapted shRNA
STE	sucrose-Tris-EDTA medium
TBS	Tris-buffered saline
TMPD	*N,N,N′,N′*-tetramethyl-*p*-phenylenediamine
TMRM	tetramethylrhodamine methyl ester
tRNA	transfer ribonucleic acid
UTR	untranslated region

ABSTRAKT

Savčí organismus je plně závislý na systému oxidativní fosforylace (OXPHOS) jako hlavním zdroji produkce energie (ATP) v buňce. Poruchy OXPHOS mohou být způsobeny mutacemi v genech kódovaných mitochondriální DNA nebo jadernou DNA.

Část výzkumné práce je zaměřena na roli raně a pozdně se asemblujících, jaderně kódovaných, strukturních podjednotek cytochrom c oxidasy (CcO) a Oxa1l, lidského homologu kvasinkové mitochondriální Oxa1 translokasy, v biogenezi cytochrom c oxidasy a její funkci s využitím stabilní RNA interference COX4, COX5A, COX6A1 a OXA1L a ektopické exprese epitopově značených podjednotek Cox6a, Cox7a a Cox7b v buněčné linii HEK (lidské embryonální ledviny)-293. Naše výsledky ukazují, že zatímco podjednotky Cox4 a Cox5a jsou nezbytné pro asemblaci funkčního komplexu CcO, Cox6a podjednotka je důležitá pro její stabilitu. V buňkách se sníženou expresí OXA1L byla překvapivě zjištěna normální aktivita i hladina holoenzymu CcO, přestože inaktivace OXA1 u kvasinek vyvolá kompletní ztrátu aktivity CcO.

Při studiu poruch OXPHOS v izolovaných mitochondriích kosterního svalu, srdce, jater a frontálního kortexu získaných od pacientů s Leigh syndromem (mtDNA mutace 8363G>A), MERRF syndromem (mtDNA mutace 8344A>G) a MELAS syndromem (mtDNA mutace 3243A>G) jsme nalezli tkáňově specifické rozdíly v dopadu mt-tRNA mutací na OXPHOS mozku, které se významně lišily od dopadu těchto mutací v ostatních tkáních. Navíc jsme ukázali, že v případě mtDNA mikrodelece 9205ΔTA v ATP6 genu je výrazně omezena syntéza podjednotky a komplexu ATPasy a postižena biogeneze CcO.

Klíčová slova: mitochondrie, cytochrome c oxidasa, ATP synthasa (ATPasa), tkáňová specifita, asemblace proteinů, biogeneze, RNA interference (RNAi)

ABSTRACT

The mammalian organism fully depends on the oxidative phosphorylation system (OXPHOS) as the major energy (ATP) producer of the cell. Disturbances of OXPHOS may be caused by mutations in either mitochondrial DNA (mtDNA) or nuclear DNA (nDNA).

One part of the thesis is focused on the role of early and late assembled nuclear-encoded structural subunits of cytochrome c oxidase (CcO) as well as Oxa1l, the human homologue of the yeast mitochondrial Oxa1 translocase, in the biogenesis and function of the human CcO complex using stable RNA interference of COX4, COX5A, COX6A1 and OXA1L, as well as expression of epitope-tagged Cox6a, Cox7a and Cox7b, in HEK (human embryonic kidney)-293 cells. Our results indicate that, whereas nuclear- encoded CcO subunits Cox4 and Cox5a are required for the assembly of the functional CcO complex, the Cox6a subunit is required for the overall stability of the holoenzyme. In OXA1L knockdown HEK-293 cells, intriguingly, CcO activity and holoenzyme content were unaffected, although the inactivation of OXA1 in yeast was shown to cause complete absence of CcO activity.

In addition, we compared OXPHOS protein deficiency patterns in mitochondria from skeletal muscle, heart, liver and frontal cortex of patients with Leigh (mtDNA mutation 8363G>A), MERRF (mtDNA mutation 8344A>G), and MELAS (mtDNA mutation 3243A>G) syndromes. Our data show new effects of mt-tRNA mutations on the brain which differ substantially from those described for other tissues. Furthermore, we found that mtDNA 9205ΔTA microdeletion in the ATP6 gene prevents the synthesis of ATPase subunit a and also affects the biogenesis of CcO.

Key words: mitochondria, cytochrome c oxidase, ATP synthase (ATPase), tissue specificity, protein assembly, biogenesis, RNA interference (RNAi)

1 INTRODUCTION

1.1. Mitochondria

Mitochondria are the endosymbiotic semiautonomous ATP-generating organelles of eukaryotes which display striking interspecies and inter-tissue variations in shape, connectivity, and inner membrane morphology [1]. The general structure of mitochondrion is defined by its two membranes [2,3]. A topologically simple and limiting outer membrane enwraps the energy-transducing inner membrane whose surface area is considerably larger and which in turn encloses a protein-rich matrix. To accommodate the volume constraint imposed by the outer membrane, the inner membrane has numerous invaginations, the cristae, each of which can have one or more tubular connections to the membrane periphery [4]. In addition to the scaffold function of the inner membrane for the assembly and operation of the respiratory chain complexes, this highly pleomorphic structure provides the permeability barrier across which the respiratory machinery generates its chemiosmotic gradient. Electron tomographic analyses of various mitochondria provided overwhelming evidence that cristae are not simply random folds in the inner membrane but rather internal compartments formed by invaginations of the membrane, which originates at narrow neck-like segments referred as crista junctions [4-6]. The number of crista junctions and the morphology of the intercristal space have been shown to change with the metabolic state of the mitochondria [6-8] and can only be achieved by the inner membrane undergoing fusion and fission [9]. The relative activities of proteins involved in mitochondrial fusion and fission determine an overall morphology, integrity and turnover of the mitochondrial population as well as segregation and protection of mitochondrial DNA [10-13]. In many cases, mitochondria form a complex reticulum that interacts with other cellular components, in particular the cytoskeleton and endoplasmic reticulum [14,15]. Interaction of mitochondrial and endoplasmic reticulum networks and the connectivity state of mitochondria controls metabolic flow, production of reactive oxygen species (ROS), protein transport, intracellular Ca^{2+} signaling and cell death [16-20].

1.2. System of oxidative phosphorylation

ATP production in eukaryotes from glucose and oxygen normally consists of two catabolic processes [21]. First, the glycolytic system supplies mitochondria with pyruvate. Second, pyruvate dehydrogenase complex and Krebs cycle catalyze oxidative conversion of pyruvate to H_2O and CO_2. Substrates of Krebs cycle do not come only from glycolysis, but

also from beta-oxidation of fatty acids and proteolysis. Concomitantly to these catabolic processes, electrons are transferred via coenzymes NAD^+ and FAD to pass into the mitochondrial electron-transport chain which produces a proton gradient across the mitochondrial membrane. The free energy stored in this electrochemical gradient drives the synthesis of ATP from ADP and phosphate through oxidative phosphorylation [21,22]. The mechanistic principle of oxidative phosphorylation was first proposed by Peter Mitchell [23] who received for chemiosmotic hypothesis Nobel prize in 1978.

1.2.1. Electron-transport chain

Electrons travel from NADH and $FADH_2$ to O_2 through series of redox centers from lower to higher standard reduction potentials, so that the overall process is exergonic. Some of these redox centers are mobile, and others are components of integral membrane protein complexes. The released energy is used at three locations within the chain (CI, CIII and CIV) to expel protons from the matrix into the IMS, resulting in a potential difference ($\Delta\Psi$) and proton gradient (ΔpH) across the IMM [21]. The energy stored in this electrochemical proton gradient, generally referred to as proton motive force (PMF) can be used for chemical, osmotic and mechanical work. The PMF is dominated by $\Delta\Psi$, with ΔpH contributing ~15% to its total magnitude [24,25].

1.2.2. Complex V and transporters of its substrates

Complex V, F_1F_o-ATP synthase or F-type ATPase is multisubunit enzyme nearly ubiquitous in the cell membranes of eubacteria, inner membranes of mitochondria and tylakoid membranes of chloroplasts [26]. Under oxidative conditions, this enzyme synthesizes the vast majority of cellular ATP from ADP and P_i at the expense of proton or sodium motive force [27-30]. To be utilized for oxidative phosphorylation, ADP as well as inorganic phosphate (Pi) must be transported into the mitochondrial matrix. Since these substrates are large, hydrophilic, highly charged molecules, averse to low dielectric membrane environment, their transport through biomembranes requires carriers. The protein, which mediates transmembrane efflux of ATP in exchange for ADP, is ADP/ATP carrier [31]. Regarding inorganic phosphate, its smaller fraction may be transported by the dicarboxylate carrier, which catalyzes a Pi/dicarboxylate or Pi/Pi exchange. However, the protein, which is mainly responsible for phosphate transport, is the mitochondrial phosphate carrier [32].

1.3. Mitochondrial disorders

As mentined above, mitochondria hold a central position in cellular bioenergetics. The importance of mitochondria for cell viability is most dramatically apparent from diseases resulting from its malfunction. OXPHOS disorders, first recognized 50 years ago [33], have been found to be the most frequent cause of metabolic abnormality in pediatric neurology [34,35] but often present with nonneurological symptoms (e. g. hepatic, cardiac, renal, gastrointestinal, endocrine, hematological symptoms, failure to thrive) [36,37] or can contribute to severe diseases of adulthood (e. g. Parkinson's disease, Alzheimer's disease, Type 2 diabetes mellitus) [38-40]. The clinical and genetic variability of OXPHOS disorders makes it extremely difficult to estimate prevalence accurately; however, the general incidence of mitochondrial disease is approximately 1:5000 [41,42]. Since the OXPHOS is composed of 13 structural subunits encoded by mtDNA and more than 70 structural polypeptides encoded by nDNA, primary OXPHOS disorders can be classified genetically according to whether the primary defect is in the nuclear or mitochondrial genome. Furthermore, 24 additional mtDNA-encoded genes are involved in mitochondrial translational apparatus and numerous nDNA-encoded genes are necessary for synthesis of prosthetic groups and assembly of OXPHOS complexes, stability of mtDNA and mitochondrial biogenesis. Therefore, inheritance of these mutations may be autosomal recessive or dominant, X-linked or maternal [43].

At the metabolic level, the impact of OXPHOS disease can be classified as systemic consequences (e. g. pathological increase in concentration of the lactic acid, alanin or higher ketone body ratio) or consequences at the tissue and cellular level (bio-energy deficiency, redox or metabolite imbalance or elevated or disturbed production of ROS) [44]. Biochemically, OXPHOS defects are classified based on the affected enzyme as isolated (only one OXPHOS enzyme is deficient) or combined (more than one complex deficiency is observed). Due to high complexity of genes which are involved in optional functioning of OXPHOS, some of which very likely remain to be identified, most patients are still classified clinically or biochemically, simply because the genetic defect has not yet been established. Therefore, there is a great need to better understand the genetics of mitochondrial disease as well as biogenesis of OXPHOS, which will enable prenatal diagnoses and will deliver deeper understanding of mitochondrial function necessary for development of effective therapies [45].

2 AIMS OF THE STUDY

Our laboratory for study of mitochondrial disorders specializes in biochemical and molecular diagnostics of OXPHOS deficiencies in the patients predominantly coming from Czech and Slovak Republics. One part of this thesis is based on the study of selected deleterious mutations of mtDNA in terms of their impact on OXPHOS steady-state levels and functioning in various patients´ tissues. All analyzed mutations, especially those in genes coding for mt-tRNAs, usually affects more than one OXPHOS complex, thus they manifest as combined OXPHOS defects. We were interested in differences in OXPHOS deficiency patterns among various tissues.

Second part of this thesis is aimed at biogenesis of cytochrome c oxidase (CcO), the complex IV of OXPHOS, which plays central role in oxidative metabolism. Defective CcO functionality results in heterogeneous group of diseases predominantly affecting tissues with high-energy demands. In the group of 180 CcO-deficient children identified in Poland, Czech and Slovak Republics [46], molecular basis of CcO deficiency, which is fundamental e. g. for prenatal diagnostics in affected families, still remains to be elucidated approximately in the half of cases. Therefore, the study of CcO biogenesis also became an important interest in our laboratory and of my thesis.

The specific aims of this thesis have been:

1) ***to study new aspects of the CcO assembly pathway***
   a) Characterization of the assembly and function of human nuclear-encoded CcO subunits 4, 5a, 6a, 7a and 7b.
   b) Characterization of the biochemical properties of OXA1L, the human homologue of the yeast mitochondrial Oxa1 translocase, and study of its role for CcO biogenesis.
2) ***to study the molecular basis of selected mtDNA-encoded mutations and their impact on OXPHOS function***
   a) Analysis of the tissue-specific effects of mt-tRNA point mutations in patients affected by Leigh syndrome (8363G>A), MERRF syndrome (8344A>G), and MELAS syndrome (3243A>G) on the steady-state levels and activity of OXPHOS complexes.
   b) Study of molecular and biochemical impact of mtDNA mutation in the ATP6 gene (9205ΔTA) on the biosynthesis of ATPase subunit a and its structural and functional consequences.

3 MATERIAL AND METHODS

3.1. Tissues and cell lines

Human samples for analyses were obtained from patients with mtDNA microdeletion 9205ΔTA, from three patients harboring two mutations in mt-tRNA^{Lys} (8363G>A and 8344A>G) or one mutation in mt-tRNA$^{Leu(UUR)}$ (3243A>G), as well as from age-related controls. Open muscle biopsies from the tibialis anterior muscle were frozen at -80°C. Post-mortem tissue specimens obtained at autopsy of patients with mtDNA mutations 8363G>A and 3243A>G, and controls were frozen less than 2 h after death. Fibroblast cultures were established from skin biopsies. HEK-293 cells (CRL-1573) were obtained from A.T.C.C. (Manassas VA, U.S.A.).

3.2. Ethics

All studies were carried out in accordance with the Declaration of Helsinki of the World Medical Association and were approved by the Committees of Medical Ethics at all collaborating institutions. Informed consent was obtained from investigated individuals or their parents.

3.3. Plasmid construction

The nucleotide sequences of 41 different candidate shRNAmirs targeted to COX4I1, COX5A, COX6A1 and OXA1L mRNAs were designed with shRNA Retriever (http://katahdin.cshl.org/ siRNA/RNAi.cgi?type=shRNA) or downloaded from the publicly accessible RNAi Codex database [47]. The corresponding 97-mer oligonucleotides were synthesized (Invitrogen) and used as template sequences for PCR amplification to produce clonable double-stranded XhoI/EcoRI restriction fragments which were inserted into pCMV-GIN-Zeo vector (Open Biosystems). The negative control (non-silencing) shRNAmir pCMV-GIN-Zeo derivative was obtained from Open Biosystems. The coding sequences of COX7A2 (IMAGE ID: 40002220) and COX7B (IMAGE ID: 3861730) were amplified from the respective full-length cDNA clones (ImaGenes), fused to the C-terminal FLAG epitope and cloned (EcoRI/NotI) into the modified pmaxFP-Red-N plasmid (Amaxa). The full length human OXA1L coding sequence (IMAGE ID: 40017377) was amplified and inserted into the C-FLAG fusion mammalian expression vector pCMV-Tag4a (Stratagene). The fidelity of all constructs was confirmed by automated DNA

sequencing. Plasmids pReceiver-M02 (EXC0224) and pReceiver-M13 (EX-C0224) (GeneCopoeia) were used to express Cox6a2 and Cox6a2–FLAG respectively.

3.4. Cell cultures, transfections and flow cytometry

Fibroblast cultures and HEK-293 cells were grown in Dulbecco's modified Eagle's medium supplemented with 10% (v/v) fetal calf serum (Sigma) and fetal bovine serum Gold (PAA), respectively, at 37°C in 5% CO_2. HEK-293 cell lines stably expressing shRNAmir were prepared using the Nucleofector™ device (Amaxa) and the HEK-293 cell-specific transfection kit. At 48 h after the transfection, antibiotic-resistant colonies were selected and further maintained in the presence of 720 μg/ml G418 (Clontech). The GFP fluorescence of stable G418-resistant HEK-293 cells was measured with a FACSCalibur flow cytometer and analyzed using the Cell Quest 3.3 application (Becton Dickinson).

The transient expression of Oxa1l or selected CcO subunits in HEK-293 cells was accomplished using the Lipofectamine 2000 reagent (Invitrogen) or the Express-In Transfection Reagent (Open Biosystems). To obtain optimal accumulation of the CcO subunit polypeptides, the cells were transfected twice consecutively, leading to transgene expression for a total of 4 days. To assess the efficiency of the shRNAmir constructs interfering with *OXA1* transcripts, HEK-293 cells were co-transfected using a Nucleofector™ device with either one of the eight OXA1L-targeted shRNA constructs or the negative control (non-silencing) shRNA construct and with the OXA1L-FLAG expression construct. At 48 h after the transfection, the cells were lysed and the expression level of the Oxa1l-FLAG fusion protein was examined by immunoblot analysis.

3.5. Isolation of mitochondria

Mitochondria from fibroblasts were isolated by a hypo-osmotic shock method [48]. Mitoplasts from fibroblasts were prepared as described previously [49]. To isolate mitochondria from HEK-293 cells, collected and thawed cells were resuspended in STE buffer [250 mM sucrose, 10 mM Tris/HCl (pH 7.4), 1 mM EDTA, 1% (w/v) Protease inhibitor cocktail (Sigma)], homogenized in a glass/glass homogenizer at 4°C. Unbroken cells and nuclei were removed by centrifugation for 15 min at 4°C and 600 g and the mitochondrial fraction was isolated from the postnuclear supernatant by centrifugation for 25 min at 4°C and 10 000 g. The mitochondrial pellet was washed, resuspended in STE buffer (2.5 volume of the mitochondrial pellet) and stored at -80°C. Muscle mitochondria

were isolated according to [50], but without use of protease. The mitochondrial pellet was stored at a final protein concentration of 20-25 mg/ml at -80°C.

3.6. Immunofluorescence

HEK-293 cells (1.5×10^5) grown on 70 mm^2 glass chamber slides (BD Falcon) were transfected with an OXA1L–FLAG expression construct using the Lipofectamine 2000 reagent. At 24 h after the transfection, the cells were incubated with 200 nM MitoTracker Red CMX Ros (Molecular Probes) for 15 min, and then fixed and permeabilized with PBS containing 4% (v/v) paraformaldehyde and 0.1% (v/v) Triton X-100 solutions, respectively. Subsequently, the cells were incubated in PBS with 10% (w/v) BSA for 1 h at 37°C to block non-specific binding. Immunocytochemical detection was then performed with a monoclonal M2 anti-FLAG and with an anti-mouse IgG_1 Alexa Fluor® 488 antibody.

3.7. Laser scanning confocal microscopy

xyz images sampled according to the Nyquist criterion were acquired using a Nikon Eclipse TE2000 microscope equipped with a C1*si* confocal scanning head and an Apo TIRF 60× (N.A. 1.49) objective. The 488 nm and 543 nm laser lines and appropriate 515±15 and 590±15 nm band pass filter sets were used for excitation and fluorescence detection, respectively. Individual channel images were acquired separately. Images were restored using the measured point spread function (PSF) and the classic maximum likelihood deconvolution algorithm in Huygens Professional Software (SVI).

3.8. Sub-cellular and submitochondrial fractionation

The postnuclear supernatant from isolation of HEK-293 mitochondria was centrifuged at 10 000 g for 25 min. The resulting supernatant corresponding to the cytoplasmic fraction was collected, and the mitochondrial pellet was washed once with the STE buffer. For sonical disruption, isolated mitochondria were adjusted to a protein concentration of 2.5 mg/ml, sonicated and centrifuged at 100 000 g for 30 min. Alkaline sodium carbonate extraction of mitochondrial membranes was performed essentially as described [51].

3.9. Preparation of a polyclonal antibody to human Oxa1l

An Oxa1l-specific antibody was prepared by Open Biosystems. An Oxa1l-specific antiserum was generated by immunizing chicken with a synthetic peptide (KLH-coupled)

corresponding to the C-terminal part of human Oxa1l (CKPKSKYPWHDT). The polyclonal antibody to human Oxa1l was affinity-purified from the total IgY with the respective peptide-packed column. The specificity of the produced antibody was tested by immunodetection of the Oxa1l-FLAG fusion protein.

3.10. Electrophoresis and Western blot analysis

In cultured skin fibroblasts, mitoplasts were solubilized using 1 g of DDM/g of protein and OXPHOS complexes were separated on 6-15% (w/v) polyacrylamide gradient BN-PAGE [50] minigels (Mini Protean system; Bio-Rad) as described previously [49]. SDS/PAGE [52] was performed on 10% (w/v) polyacrylamide slab minigels, and analysis of [^{35}S] methionine-labelled proteins was performed on a 16 cm long 15-20% (w/v) gradient polyacrylamide slab gels (Protean system; Bio-Rad). For 2D analysis, strips of the first-dimension BN-PAGE gel were incubated for 1 h in 1% (w/v) SDS and 1% (v/v) mercaptoethanol and then subjected to second dimension SDS/PAGE (10% polyacrylamide) [52]. For analysis of respiratory supercomplexes by BN/SDS/PAGE and BN/BN/PAGE, isolated mitochondria were extracted using digitonin (detergent/protein ratio of 6).The first dimension gel strips for BN/BN/PAGE immunodetection were soaked in cathode buffer containing 0.1% DDM for 15 min and then in cathode buffer containing 0.02% DDM for another 15 min. The second dimension of BN-PAGE separation was performed in the presence of 0.02% DDM as described in [53]. Gels were blotted onto Hybond C-extra nitrocellulose membranes (Amersham) or Immobilon™-P PVDF membranes (Millipore) by semi-dry electrotransfer for 60-90 min at a constant current of 0.6-0.8 mA/cm^2. Membranes were air-dried overnight, rinsed twice with 100% (v/v) methanol, and blocked in PBS containing 0.2% (v/v) Tween 20 or in TBS containing 10% (w/v) non-fat dried milk for 1-3 h.

For primary detection of OXPHOS complexes or individual subunits, antibodies raised against complex I subunit NDUFA9, NADH39 and NDUFB6; complex III subunit Core1, Core2; complex IV subunit Cox1, Cox2, Cox4, Cox5a, Cox6a1, Cox6c; complex II subunit 70 kDa protein; the ATP synthase subunit F1-α, F1-β, d, OSCP, F_oc or F_oa (ATP6) [54,55]; pyruvate dehydrogenase (PDH) subunit E2; mtHSP70 protein; α-tubulin; eIF2α and anti-FLAG were used. Secondary detection was carried out with a goat anti-mouse or anti-rabbit IgG-horseradish peroxidase conjugate in TBS, 0.1-0.2% Tween 20 and 2% (w/v) non-fat dried milk or BSA, for 1 h. The immunoblots were developed with ECL® kit (Amersham) or SuperSignal West Femto Maximum Sensitivity Substrate (Pierce). Signal

acquisition was performed using LAS 1000 instrument (Fuji), VersaDoc 4000 imaging system (Bio-Rad Laboratories) or Kodak BioMax Light films (Eastman Kodak Co.). Digital images were analyzed using the Quantity One application (Bio-Rad Laboratories) or Aida 2.11 Image Analyzer software.

3.11. Immunoprecipitation of Oxa1l–FLAG protein

HEK-293 cells (~10^6) were transiently (48 h) transfected with the Oxa1l–FLAG expression construct, lysed with a buffer containing 1% Triton X-100, 150 mM NaCl, 1 mM EDTA and 50 mM Tris/HCl (pH 7.4), and the lysate was incubated for 6 h at 4°C with previously washed 50 µl of an ANTI-FLAG® M2 affinity agarose resin (flagipt-1; Sigma). Subsequently, the resin was washed five times with a buffer containing 150 mM NaCl, 50 mM Tris/HCl (pH 7.4), and the bound protein was eluted by competition with 3×FLAG peptide. Finally, the eluted immunoprecipitate was combined with SDS sample buffer and resolved using SDS/PAGE.

3.12. Spectrophotometric assays

The activities of respiratory chain complexes were measured spectrophotometrically with a UV-2401PC instrument (Shimadzu). The activities of the mitochondrial enzymes NADH:coenzyme Q_{10} reductase (NQR, complex I), succinate:coenzyme Q_{10} reductase (SQR, complex II), succinate:cytochrome c reductase (SCCR, complex II+III), NADH:cytochrome c reductase (NCCR, complex I+III), coenzyme Q_{10}:cytochrome c reductase (QCCR, complex III), and cytochrome c oxidase (COX, CcO, complex IV) were measured spectrophotometrically by standard methods at 37°C in muscle homogenate and isolated muscle mitochondria [56,57], in cultured fibroblasts [58] or HEK-293 mitochondria [59]. The total protein was determined using the method of Lowry [60]. Aurovertin-sensitive ATP hydrolytic activity was measured in a ATP-regenerating system as described in [61].

3.13. High-resolution oxygraphy

Oxygen consumption in cultured fibroblasts was determined at 30°C as described in [58,62] using an Oxygraph-2k (Oroboros) and expressed in pmol of oxygen/s per mg of protein. Muscle fibers were separated mechanically according to [63], and oxygen consumption by saponin-skinned muscle fibers was determined as described [64].

The oxygen consumption of digitonin-permeabilized HEK-293 cells was measured at 30°C in a medium containing 0.5 mM EGTA, 3 mM $MgCl_2$, 60 mM potassium lactobionate, 20 mM taurine, 10 mM KH_2PO_4, 110 mM sucrose, 1 g/l BSA, 20 mM Hepes (pH 7.1). The measurements were carried out in the presence of 30-75 μg/ml of digitonin, 2.5 μM antimycin A, 2 mM ascorbate, 500 μM TMPD and 0.5-1.5 μM FCCP. Respiration was inhibited by the addition of sodium azide to a final concentration of 10 mM. The P_{50} (partial pressure of oxygen at the half-maximal respiration rate) value was measured in the presence of 0.5 μM FCCP and 10 mM succinate essentially as described in [65]. All measurements were performed independently three to six times for each cell line.

3.14. Cytofluorimetric analysis of mitochondrial membrane potential

Freshly harvested fibroblasts were resuspended in 80 mM KCl, 10 mM Tris/HCl (pH 7.4), 3 mM $MgCl_2$, 1 mM EDTA, 5 mM potassium phosphate and 10 mM succinate at a protein concentration of 1 mg/ml. Cells (~ 10^4 per each measurement) were permeabilized by 0.1 mg digitonin per mg protein (Sigma) and stained with 20 nM TMRM (Molecular Probes) for 15 min at room temperature. ADP, inhibitors, or both were added at indicated concentrations 1 min before cytofluorometric measurements, which were performed as described elsewhere [66] on a FACSort flow cytometer (Becton Dickinson) equipped with an argon laser, 488 nm. The TMRM signal was analyzed in the FL2 channel, equipped with a band pass filter 585±21 nm; the photomultiplier value of the detector was at 631 V in FL2. Data were acquired in log scale using CellQuest (Becton Dickinson) and analyzed with WinMDI 2.8 software (TSRI). Arithmetic mean values of the fluorescence signal in arbitrary units were determined for each sample for the purpose of subsequent graphic representation.

3.15. ATP synthesis

The rate of ATP synthesis was measured at 37°C in 150 mM KCl, 25 mM Tris/HCl, 10 mM potassium phosphate, 2 mM EDTA and 1% (w/v) BSA, pH 7.2, using 0.5 mM ADP and 10 mM succinate or 10 mM pyruvate + 10 mM malate (or ketoglutarate + malate) as substrate according to [67]. Protein concentration was 1 mg/ml. For permeabilization of fibroblasts and cybrids, 0.1 and 0.03 mg of digitonin/mg of protein, respectively, was used. The reaction was started by addition of the cells and performed for the indicated time intervals. Reaction mixture aliquots of 200 μl were added to 200 μl of DMSO, and ATP

content was determined in DMSO-quenched samples by a luciferase assay according to [68]. ATP production was expressed in nmol of ATP/min per mg of protein.

3.16. Biosynthesis of mitochondrial proteins

Growth medium was removed from cultured fibroblasts, and the cells were rinsed with methionine-free medium without serum (Gibco medium 21013; 1 mM pyruvate, 2 mM glutamine and 30 mg/l cysteine) and incubated in the same medium containing 10% (v/v) dialysed fetal calf serum and 100 μg/ml emetine for 10 min. The cells were labelled for 3 h with 300 μCi/ml L-[^{35}S] methionine, as described in [69]. The products were separated by 15–20% (w/v) polyacrylamide gradient SDS/PAGE. A small aliquot of the samples prepared for electrophoresis was used to measure the total incorporation of radioactivity in the mitochondrial fraction as trichloroacetic acid-precipitable counts. The radioactivity of proteins was quantified in dried gels using a BAS-5000 system (Fuji). Labelled proteins were identified according to their molecular mass as reported previously in *ex vivo* translation assays [69].

3.17. Protein determination

The protein content was measured by the Bradford or Micro BCA protein kit assays (Bio-Rad Laboratories), using BSA as a standard. Samples were sonicated for 20 s prior to protein determination.

3.18. DNA analysis and sequencing

Total genomic DNA from muscle and cultured fibroblasts was isolated by phenol extraction. The entire mtDNA was amplified in six overlapping fragments by PCR (7-3148, 2073-5719, 5645-8815, 8403-11 132, 11 005-14 684 and 13 863-136). Purified fragments were sequenced on the automatic sequencer ALF Express II (Amersham Biosciences) using cycle sequencing with 41 Cy5-labelled internal sequencing primers or on an AbiPrism 3100 Avant Genetic Analyzer (Applied Biosystems).

3.19. Restriction analysis

To determine the amount of mtDNA mutations, PCR/RFLP (restriction fragment length polymorphism) analysis method was performed. 9205delTA microdeletion was quentified according to [70]. To quantify 8363G>A mutation, PCR products (8279-8485)

were radioactively labelled with [α-^{32}P] dCTP in the final cycle of PCR, and run on a non-denaturing 10% (w/v) polyacrylamide gel after complete digestion with TspRI (New England BioLabs). The mutation abolishes one of two TspRI restriction sites on the fragment. The levels of heteroplasmy of the prevalent 3243A>G and 8344A>G mutations were determined as described elsewhere [71]. The proportions of wild-type to mutant mtDNA were measured using PhosphorImager and ImageQuant software (Molecular Dynamics).

3.20. Northern blot analysis

Total RNA was isolated from cultured fibroblasts by phenol/guanidium thiocyanate/chloroform extraction [72]. ~20 μg of total RNA per lane was separated through a 1.2% (w/v) agarose/formaldehyde gel and transferred to a Hybond-N nylon membrane (Amersham) in 20×SSC (1×SSC is 0.15 M NaCl/ 0.015 M sodium citrate). The membrane was prehybridized for 2 h at 45°C in 5×SSC, Denhardt's solution, 0.5% SDS and 100 μg/ml sonicated herring sperm. The membranes were hybridized overnight at 45°C with [α-^{32}P] dCTP-labelled probes corresponding to regions of the genes ATP6 (8361-9060), COX3 (9269-9912), ND1 (3313-4252) and COX1 (6120-6960). The radioactivity was detected by PhosphorImager and ImageQuant software (Molecular Dynamics).

3.21. Quantitative RT-PCR (reverse transcription–PCR) analysis

Total RNA was isolated using RNA Blue reagent (Top-Bio) or TriReagent solution (MRC). Following DNase I treatment (Invitrogen), first-strand cDNA was synthesized from 1-4 μg of total RNA with SuperScript II or III reverse transcriptase and random hexamer or Oligo-dT primers (all Invitrogen or Promega) according to the manufacturer's instructions. Real-time quantitative RT-PCR of cDNA was performed on a LightCycler instrument (Roche Diagnostics) using a QuantiTect SYBR Green PCR kit (Qiagen) by amplification of fragments specific for *ATP6* (nt 8846-8994), *COX3* (nt 9267-9416), *ATP6–COX3* (nt 9150-9299), *CYTB* (nt 14 804-14 935) and *ND1* (nt 3595-3644) transcripts. The primer pair for ATP6–COX3 was designed to flank the splice site of the *ATP6–COX3* transcript. Amplified regions of the *ATP6* or *COX3* transcript were present in both processed and unprocessed RNAs. To quantify isoforms of CcO structural subunits, pre-amplification (10 cycles) and relative quantification was performed according to the manufacturer's instructions (Applied Biosystems) with eight TaqMan Gene Expression Assays specific for

COX4I1, *COX4I2*, *COX6A1*, *COX6A2*, *TBP* (TATA-box-binding protein), *PPARGC1A* (peroxisome-proliferator-activated receptor γ co-activator 1α), *SDHA* (succinate dehydrogenase complex subunit A) and *TFAM* (transcription factor A, mitochondrial) transcripts. Relative quantification was performed on the 7300 Real-Time PCR System (Applied Biosystems) by comparative $\Delta\Delta C^t$ method. The transcript levels of all mRNAs were normalized to the level of *TBP* mRNA. All reactions were performed in triplicate and each sample was analyzed in two separate experiments.

3.22. Statistical analysis

A Student's t test was performed using Microsoft Excel. Results are expressed as mean±S.D. A *P* value of less than 0.05 was considered as statistically significant, and asterisks are used to denote significance as follows: **P*<0.05; ** *P* <0.01; *** *P* <0.001.

4 RESULTS AND DISCUSSION

4.1. Characterization of the assembly and function of human nDNA-encoded CcO subunits 4, 5a, 6a, 7a and 7b *(specific aim 1a)*

Fornuskova D, Stiburek L, Wenchich L, Vinsova K, Hansikova H and Zeman J. Novel insights into the assembly and function of human nuclear-encoded cytochrome *c* oxidase subunits 4, 5a, 6a, 7a and 7b. **Biochem J** 2010; 428: 363-374.

To study the role of nuclear-encoded cytochrome c oxidase (CcO) structural subunits Cox4, Cox5a and Cox6a as well as the sequence of late events in the CcO assembly pathway, we prepared stable HEK-293 knockdown lines using microRNA-adopted design evoking RNA interference of *COX4*, *COX5A* and *COX6A1*. Furthermore, we used ectopic expression of C-end epitope-tagged Cox6a, Cox7a and Cox7b in wild-type HEK-293 cells and COX6A knockdowns to elucidate entry points of these subunits into the CcO assembly pathway. To estimate functionality and integrity of OXPHOS in context of CcO deficiency, we employed quantitative real-time RT-PCR, isolation of crude mitochondrial fraction by cellular fractionation and differential centrifugation, spectrophotometric enzyme activity assays, high-resolution respirometry and blue-native (BN), denaturing (SDS) and two-dimensional (BN/SDS or BN/BN) PAGE with downstream immunoblot detections using monoclonal antibodies against various mitochondrial proteins.

Knockdown of Cox4, Cox5a and Cox6a resulted in reduced CcO activity, diminished affinity of the residual enzyme for oxygen, decreased CcO holoenzyme and CcO dimer levels, increased accumulation of CcO subcomplexes and gave rise to an altered pattern of respiratory supercomplexes. An analysis of the patterns of CcO subcomplexes found in both knockdown and overexpressing cells identified a novel CcO assembly intermediate, identified the entry points of three late-assembled subunits and demonstrated directly the essential character as well as the interdependence of the assembly of Cox4 and Cox5a. The ectopic expression of the heart/muscle-specific isoform of the Cox6 subunit (COX6A2) resulted in restoration of both CcO holoenzyme and activity in COX6A1-knockdown cells. This was in sharp contrast with the unaltered levels of *COX6A2* mRNA in these cells suggesting the existence of a fixed expression programme. The normal amount and function of respiratory complex I in all of our CcO-deficient knockdown cell lines suggest that, unlike non-human CcO-deficient models, even relatively small amounts of CcO can maintain the normal biogenesis of respiratory complex I in cultured human cells.

I contributed fundamentally to this study by designing the research, cloning of pCMV-GIN-Zeo plasmid derivatives coding for candidate shRNAs to achieve the most efficient knockdown, maintaining the HEK-293 cell culture, carrying out expression cloning, preparation of knockdown cell lines and transiently transfected cellular materials, performing mitochondrial isolations and all Western blot analyses and by writing the paper.

4.2. Characterization of the biochemical properties of OXA1L, the human homologue of the yeast mitochondrial Oxa1 translocase, and study of its role for CcO biogenesis *(specific aim 1b)*

Stiburek L, **Fornuskova D**, Wenchich L, Pejznochova M, Hansikova H and Zeman J. Knockdown of human Oxa1l impairs the biogenesis of F_1F_o-ATP synthase and NADH:ubiquinone oxidoreductase. **J Mol Biol** 2007; 374: 506-516.

To study the molecular role and biochemical properties of human OXA1L gene product, we employed expression cloning and propagation of plasmid constructs in bacteria, rabbit OXA1L antibody design and preparation, immunocytochemistry, confocal microscopy, co-immunoprecipitation as well as subcellular and submitochondrial fractionation and localization. To estimate functionality and integrity of OXPHOS in context of Oxa1l deficiency, we prepared stable human HEK-293 knockdown lines using human microRNA-adopted design evoking RNA interference. The obtained material was analyzed with use of isolation of crude mitochondrial fraction by cellular fractionation and differential centrifugation, FACS analysis, spectrophotometric measurements of specific enzyme activities, high-resolution respirometry and blue-native (BN), denaturing (SDS) and two-dimensional (BN/SDS) PAGE with downstream immunoblot detections using monoclonal or polyclonal antibodies against various mitochondrial proteins.

The Oxa1 protein is a member of the evolutionarily conserved Oxa1/Alb3/YidC protein family, which is involved in the biogenesis of membrane proteins in mitochondria, chloroplasts and bacteria. The predicted human homologue, Oxa1l, was originally identified by partial functional complementation of the respiratory growth defect of the yeast oxa1 mutant. Here we demonstrate that both the endogenous human Oxa1l, with an apparent molecular mass of 42 kDa, and the Oxa1l-FLAG chimeric protein localize exclusively to mitochondria in HEK-293 cells. Furthermore, human Oxa1l was found to be an integral membrane protein, and, using two-dimensional blue native/denaturing PAGE, the majority of the protein was identified as part of a 600–700 kDa complex. The stable

short hairpin (sh) RNA-mediated knockdown of Oxa1l in HEK-293 cells resulted in markedly decreased steady-state levels and ATP hydrolytic activity of the ATP synthase and moderately reduced levels and activity of NADH:ubiquinone oxidoreductase (complex I). However, no significant accumulation of corresponding sub-complexes could be detected on blue native immunoblots. Intriguingly, the achieved depletion of Oxa1l protein did not adversely affect the assembly or activity of cytochrome c oxidase or complex III. Taken together, our results indicate that human Oxa1l represents a mitochondrial integral membrane protein required for the correct biogenesis of ATP synthase and complex I.

I contributed to this study by assisting in research design, by cloning of pCMV-GIN-Zeo plasmid derivatives coding for candidate shRNAs to achieve the most efficient knockdown and by performing the part of electrophoretic and immunoblot analyses.

4.3. Analysis of the tissue-specific effects of mt-tRNA point mutations in patients affected by Leigh syndrome (8363G>A), MERRF syndrome (8344A>G), and MELAS syndrome (3243A>G) on the steady-state levels and activity of OXPHOS complexes *(specific aim 2a)*

Fornuskova D, Brantova O, Tesarova M, Stiburek L, Honzik T, Wenchich L, Tietzeova E, Hansikova H and Zeman J. The impact of mitochondrial tRNA mutations on the amount of ATP synthase differs in the brain compared to other tissues. **Biochim Biophys Acta** 2008; 1782: 317-325.

Numerous studies have characterized the molecular mechanisms of point mutations in mitochondrial tRNA genes *in vitro*, but less was known how these mutations affect the amount and stability of OXPHOS complexes in human tissues. We have characterized the tissue- and gene-specific impact of 8363G>A, 8344A>G and 3243A>G mutations affecting mt-tRNA^{Lys} and mt-tRNA$^{Leu(UUR)}$ on OXPHOS complexes in various tissues of patients carrying these mutations with clinical phenotypes of Leigh, MERRF and MELAS syndromes.

We used spectrophotometric measurements of specific enzyme activities, high-resolution respirometry and isolation of crude mitochondrial fraction by cellular fractionation and differential centrifugation to perform blue-native (BN) and two-

dimensional (BN/SDS) PAGE with downstream immunoblot detections using monoclonal antibodies against various mitochondrial proteins.

In skeletal muscle mitochondria, both mutations that affect mt-tRNA^{Lys} (8363G>A, 8344A>G) resulted in severe combined deficiency of complexes I and IV, compared to an isolated severe defect of complex I in the 3243A>G sample (mt-tRNA$^{Leu(UUR)}$). Furthermore, we compared obtained patterns with those found in the heart, frontal cortex, and liver of 8363G>A and 3243A>G patients. In the frontal cortex mitochondria of both patients, the patterns of OXPHOS deficiencies differed substantially from those observed in other tissues, and this difference was particularly striking for ATP synthase. Surprisingly, in the frontal cortex of the 3243A>G patient, whose ATP synthase level was below the detection limit, the assembly of complex IV, as inferred from 2D-PAGE immunoblotting, appeared to be hindered by some factor other than the availability of mtDNA-encoded subunits.

I contributed to this study by designing the research, carrying out the part of one-dimensional and two-dimensional electrophoretic and immunoblot analyses, and by writing the paper.

4.4. Study of molecular and biochemical impact of mtDNA mutation in the ATP6 gene (9205ΔTA) on the biosynthesis of ATPase subunit a and its structural and functional consequences *(specific aim 2b)*

Jesina P, Tesarova M, **Fornuskova D**, Vojtiskova A, Pecina P, Kaplanova V, Hansikova H, Zeman J and Houstek J. Diminished synthesis of subunit a (ATP6) and altered function of ATP synthase and cytochrome c oxidase due to the mtDNA 2 bp microdeletion of TA at positions 9205 and 9206. **Biochem J** 2004; 383: 561-571.

To unravel the molecular basis of combined cytochrome c oxidase and ATP synthase deficiency in patient with fatal infantile encephalopathy, severe psychomotor delay, frontal lobe atrophy and lactic acidosis, we used mtDNA sequencing. We found a very rare mtDNA mutation in the ATP6 gene – a 2bp microdeletion at positions 9205 and 9206 (9205ΔTA). This mutation cancels the STOP codon of ATP6 gene and changes the cleavage site between the *ATP6* and *COX3* transcripts. The amount of mtDNA containing the microdeletion was determined by the PCR/RFLP analysis in available tissues of the patient and his relatives. The functionality and integrity of OXPHOS, especially of complexes IV and V, was studied using isolation of crude mitochondrial fraction by cellular

fractionation and differential centrifugation, spectrophotometric measurements of specific enzyme activities, rate of ATP synthesis, quantitative real-time RT-PCR and Northern blot analyses, assay for biosynthesis of mitochondrial proteins, high-resolution respirometry, cytofluorimetric analysis of mitochondrial membrane potential, and blue-native (BN), denaturing (SDS) and two-dimensional (BN/SDS) PAGE with downstream immunoblot detections using monoclonal or polyclonal antibodies against various mitochondrial proteins.

The mutation was present at increasing load in a three-generation family (in blood: grandmother - 16%, mother - 82%, proband - >98%). In the affected boy with severe encephalopathy, a homoplasmic mutation was present in blood, fibroblasts and muscle. The fibroblasts from the patient showed normal aurovertin-sensitive ATPase hydrolytic activity, a 70 % decrease in ATP synthesis and an 85 % decrease in CcO activity. ADP-stimulated respiration and the ADP-induced decrease in the mitochondrial membrane potential at state 4 were decreased by 50 %. The content of subunit a was decreased 10-fold compared with other ATPase subunits, and [^{35}S] methionine labelling showed a 9-fold decrease in subunit a biosynthesis. The content of CcO subunits 1, 4 and 6c was decreased by 30–60 %. Northern Blot and quantitative real-time reverse transcription–PCR analysis further demonstrated that the primary *ATP6–COX3* transcript is cleaved to the *ATP6* and *COX3* mRNAs 2–3-fold less efficiently. Structural studies by blue-native and two-dimensional electrophoresis revealed an altered pattern of CcO assembly and instability of the ATPase complex, which dissociated into subcomplexes. The results indicate that the 9205ΔTA mutation prevents the synthesis of ATPase subunit a, and causes the formation of incomplete ATPase complexes that are capable of ATP hydrolysis but not ATP synthesis. The mutation also affects the biogenesis of CcO, which is present in a decreased amount in cells from affected individuals.

I contributed to this study by identification of the 9205ΔTA mutation in mitochondrial genome of the patient and his relatives.

Vojtiskova A, Jesina P, Kalous M, Kaplanova V, Houstek J, Tesarova M, **Fornuskova D**, Zeman J, Dubot A and Godinot C. Mitochondrial membrane potential and ATP production in primary disorders of ATP synthase. **Toxicol Mech Methods** 2004; 14: 7-11.

We also sumarized the functional consequences of primary ATPase defects resulting from 8993T>G, 9205ΔTA and 8527A>G mutations in the ATP6 gene at the level of

mitochondrial ATP synthesis and maintenance as well as discharge of the mitochondrial membrane potential.

Studies of fibroblasts with primary defects in mitochondrial ATP synthase due to heteroplasmic mtDNA mutations in the *ATP6* gene, affecting protonophoric function or synthesis of subunit a, show that at high mutation loads, mitochondrial membrane potential $\Delta\Psi_m$ at state 4 is normal, but ADP-induced discharge of $\Delta\Psi_m$ is impaired and ATP synthesis at state 3-ADP is decreased. Increased $\Delta\Psi_m$ and low ATP synthesis is also found when the ATP synthase content is diminished by altered biogenesis of the enzyme complex. Irrespective of the different pathogenic mechanisms, elevated $\Delta\Psi_m$ in primary ATP synthase disorders could increase mitochondrial production of reactive oxygen species and decrease energy provision.

I contributed to this study by molecular analysis and preparation of cultured skin fibroblasts derived from patients.

5 CONCLUSIONS

- Whereas nDNA-encoded CcO subunits Cox4 and Cox5a are required for the assembly of the functional CcO complex, the Cox6a subunit is required for the overall stability of the holoenzyme. Consequently, the heterogeneous CcO population of Cox6a-deficient cells exhibits higher residual respiration at low oxygen levels than the various CcO forms found in COX5A-KD cells. The description of a novel assembly intermediate at the very last step of CcO assembly suggests additional regulatory level of the process.

- The fact that the ectopic expression of heart/muscle-specific isoform of Cox6a can complement the CcO defect in COX6A1-KD cells is in sharp contrast with unaltered levels of this isoform in our CcO-deficient model, and suggests the existence of a fixed differentiation programme regarding human Cox6a isoforms. The normal amount and function of complex I in all of our CcO-deficient cell lines suggest that even relatively small residual amounts of CcO can maintain normal biogenesis of this respiratory complex in human cells.

- The RNAi knockdown of OXA1L in HEK-293 cells showed that the protein plays an important role in the biogenesis of ATP synthase and respiratory complex I. In sharp contrast to the yeast orthologue, the loss of human Oxa1l does not lead to any impairments of assembly of CcO or the complex III, suggesting functional divergence during evolution.

- In skeletal muscle tissue, comparably high mutant loads (~ 90%) of 3243A>G affecting mt-tRNA$^{Leu(UUR)}$ and 8344A>G affecting mt-tRNA^{Lys} have been associated with severe defect of complex I, but only 8344A>G mutation resulted in severe deficiency of complex IV. Similarly, 80% heteroplasmy of 8363G>A mutation affecting mt-tRNA^{Lys} resulted in combined severe deficiency of complexes I and IV. Virtually the same patterns of OXPHOS holoenzyme deficiencies were observed in heart mitochondrial samples. However, the patterns of OXPHOS deficiencies in frontal cortex mitochondria of 8363G>A and 3243A>G patients differed substantially from those of other tissues. This difference was particularly striking for ATP synthase. Although it is necessary to analyze

considerably more samples with high levels of heteroplasmy (such samples are difficult to obtain), effects of mt-tRNA mutations on the brain OXPHOS are likely to be particularly different from those described for skeletal muscle, heart, and liver tissues.

- The mechanism by which the 9205ΔTA mutation affects mitochondrial function is associated with changes in the transcription of the ATP6 and COX3 genes and their translational competence and efficacy. The decrease in the amount of the mature *ATP6* transcript agreed well with the decreased synthesis and content of subunit a. Interestingly, the labelling of subunit 8 was increased, indicating up-regulated translation of the ATP8 gene, which precedes and partially overlaps the ATP6 gene. The translation of the *ATP8* and *ATP6* mRNAs is well described in yeast, but the structure of these genes and its regulation differs completely from that in mammalian mitochondria, where the mechanism of ATP8 and ATP6 biosynthesis is largely unknown. The question arises whether increased labelling of subunit 8 could be caused by translation of *ATP8* from an unspliced form of the *ATP8–ATP6–COX3* transcript, part of which is, according to our results, polyadenylated [cDNA synthesis with random primers and oligo(dT) primer] and could be therefore subjected to translation.

- Based on the cytofluorometric studies in cultured skin fibroblasts from patients with complex V defects, higher physiological levels of $\Delta\Psi_m$ can be expected because of low amount of enzyme or altered function of the F_o proton channel. Consequently, increased and unbalanced ROS production, rather than diminished energy provision, would be the key pathogenic process in primary ATP synthase diseases.

6 SUMMARY

In this PhD thesis, we utilized molecular approaches to manipulating the gene expression in human HEK-293 cell line and rare autoptic/bioptic tissue materials or cultured skin fibroblasts from patients with mitochondrial disorders to deal with molecular, biochemical and functional aspects of OXPHOS deficiencies.

We prepared stable HEK-293 cell lines with downregulated expression of selected structural CcO subunits (Cox4i1, Cox5a and Cox6a1) and OXA1L gene to study new aspects of the CcO assembly pathway. The obtained knockdown samples in combination with ectopic expression of C-end epitope-tagged Cox6a, Cox7a and Cox7b in wild-type HEK-293 cells and knockdown cell lines allowed us to elucidate early and very late events of CcO assembly and let us to propose new scheme of human CcO holoenzyme assembly pathway. Based on the study of OXA1L knockdown material, we showed that OXA1L is to a great extent expendable, unlike OXA1 in yeast, for CcO biogenesis.

Due to unique collection of tissues from patients with comparably high heteroplasmy of mt-tRNA mutations resulting in MELAS, MERRF and Leigh syndromes, we found that in skeletal muscle of the patients, the impact of mt-tRNA mutations seems to be gene-specific, whereas tissue-specificity of OXPHOS deficiency patterns was found among different tissues of the patients. Furthermore, we clarified at molecular and biochemical level a mechanism by which very rare mutation 9205ΔTA affects mitochondrial function. The data on complex V deficient cultured skin fibroblasts contributes to the growing idea that insufficient supply of ATP to meet cellular needs is not necessarily the only factor decisive for pathogenic processes in primary ATPase diseases but also increased and/or unbalanced ROS production might be underlying.

The data presented in this PhD thesis were published in 5 scientific journals and were reported at specialized national or international meetings.

7 REFERENCES

[1] Mannella, C.A. (2008). **Ann N Y Acad Sci** 1147, 171-9.
[2] Logan, D.C. (2006). **J Exp Bot** 57, 1225-43.
[3] Frey, T.G. and Mannella, C.A. (2000). **Trends Biochem Sci** 25, 319-24.
[4] Mannella, C.A. (2006). **Biochim Biophys Acta** 1763, 542-8.
[5] Mannella, C.A. (2006). **Biochim Biophys Acta** 1762, 140-7.
[6] Mannella, C.A., Marko, M. and Buttle, K. (1997). **Trends Biochem Sci** 22, 37-8.
[7] Hackenbrock, C.R. (1968). **Proc Natl Acad Sci U S A** 61, 598-605.
[8] Mannella, C.A., Marko, M., Penczek, P., Barnard, D. and Frank, J. (1994). **Microsc Res Tech** 27, 278-83.
[9] Mannella, C.A. et al. (2001). **IUBMB Life** 52, 93-100.
[10] Berman, S.B., Pineda, F.J. and Hardwick, J.M. (2008). **Cell Death Differ** 15, 1147-52.
[11] Chen, H. and Chan, D.C. (2005). **Hum Mol Genet** 14 Spec No. 2, R283-9.
[12] Cerveny, K.L., Tamura, Y., Zhang, Z., Jensen, R.E. and Sesaki, H. (2007). **Trends Cell Biol** 17, 563-9.
[13] Scott, S.V., Cassidy-Stone, A., Meeusen, S.L. and Nunnari, J. (2003). **Curr Opin Cell Biol** 15, 482-8.
[14] Rutter, G.A. and Rizzuto, R. (2000). **Trends Biochem Sci** 25, 215-21.
[15] Mannella, C.A. (2000). **J Bioenerg Biomembr** 32, 1-4.
[16] Giorgi, C., De Stefani, D., Bononi, A., Rizzuto, R. and Pinton, P. (2009). **Int J Biochem Cell Biol** 41, 1817-27.
[17] de Brito, O.M. and Scorrano, L. (2008). **Nature** 456, 605-10.
[18] Csordas, G. et al. (2006). **J Cell Biol** 174, 915-21.
[19] Szabadkai, G. and Rizzuto, R. (2007). **Adv Exp Med Biol** 594, 64-77.
[20] Kakkar, P. and Singh, B.K. (2007). **Mol Cell Biochem** 305, 235-53.
[21] Voet, D., Voet, J.G. and Pratt, C.W. (2006) Fundamentals of Biochemistry: Life at the Molecular Level*,* 2nd edn., John Wiley & Sons, Inc. MA.
[22] Saraste, M. (1999). **Science** 283, 1488-93.
[23] Mitchell, P. (1961). **Nature** 191, 144-8.
[24] Koopman, W.J., Distelmaier, F., Esseling, J.J., Smeitink, J.A. and Willems, P.H. (2008). **Methods** 46, 304-11.
[25] Nicholls, D. and Ferguson, S. (2002) Bioenergetics3*,* 3rd edn., Academic Press. London.
[26] Boyer, P.D. (1998). **Biochim Biophys Acta** 1365, 3-9.
[27] Meier, T., Polzer, P., Diederichs, K., Welte, W. and Dimroth, P. (2005). **Science** 308, 659-62.
[28] Pogoryelov, D., Yildiz, O., Faraldo-Gomez, J.D. and Meier, T. (2009). **Nat Struct Mol Biol** 16, 1068-73.
[29] Meier, T., Krah, A., Bond, P.J., Pogoryelov, D., Diederichs, K. and Faraldo-Gomez, J.D. (2009). **J Mol Biol** 391, 498-507.
[30] Preiss, L., Yildiz, O., Hicks, D.B., Krulwich, T.A. and Meier, T. (2010). **PLoS Biol** 8, e1000443.
[31] Klingenberg, M. (2008). **Biochim Biophys Acta** 1778, 1978-2021.
[32] Wohlrab, H. (1986). **Biochim Biophys Acta** 853, 115-34.
[33] Luft, R., Ikkos, D., Palmieri, G., Ernster, L. and Afzelius, B. (1962). **J Clin Invest** 41, 1776-804.
[34] Zeviani, M., Bertagnolio, B. and Uziel, G. (1996). **J Inherit Metab Dis** 19, 504-20.
[35] DiMauro, S. and Schon, E.A. (2008). **Annu Rev Neurosci** 31, 91-123.
[36] Munnich, A., Rotig, A., Chretien, D., Cormier, V., Bourgeron, T., Bonnefont, J.P., Saudubray, J.M. and Rustin, P. (1996). **J Inherit Metab Dis** 19, 521-7.
[37] Di Donato, S. (2009). **J Neurol** 256, 693-710.
[38] Lin, M.T. and Beal, M.F. (2006). **Nature** 443, 787-95.
[39] Zeviani, M. and Carelli, V. (2007). **Curr Opin Neurol** 20, 564-71.
[40] Civitarese, A.E. and Ravussin, E. (2008). **Endocrinology** 149, 950-4.

[41] Thorburn, D.R. (2004). **J Inherit Metab Dis** 27, 349-62.
[42] Schaefer, A.M., Taylor, R.W., Turnbull, D.M. and Chinnery, P.F. (2004). **Biochim Biophys Acta** 1659, 115-20.
[43] Smeitink, J., van den Heuvel, L. and DiMauro, S. (2001). **Nat Rev Genet** 2, 342-52.
[44] Smeitink, J.A., Zeviani, M., Turnbull, D.M. and Jacobs, H.T. (2006). **Cell Metab** 3, 9-13.
[45] Koene, S. and Smeitink, J. (2009). **J Intern Med** 265, 193-209.
[46] Bohm, M. et al. (2006). **Pediatr Res** 59, 21-6.
[47] Olson, A., Sheth, N., Lee, J.S., Hannon, G. and Sachidanandam, R. (2006). **Nucleic Acids Res** 34, D153-7.
[48] Bentlage, H.A., Wendel, U., Schagger, H., ter Laak, H.J., Janssen, A.J. and Trijbels, J.M. (1996). **Neurology** 47, 243-8.
[49] Klement, P., Nijtmans, L.G., Van den Bogert, C. and Houstek, J. (1995). **Anal Biochem** 231, 218-24.
[50] Schagger, H. and von Jagow, G. (1991). **Anal Biochem** 199, 223-31.
[51] Fujiki, Y., Hubbard, A.L., Fowler, S. and Lazarow, P.B. (1982). **J Cell Biol** 93, 97-102.
[52] Schagger, H. and von Jagow, G. (1987). **Anal Biochem** 166, 368-79.
[53] Wittig, I., Braun, H.P. and Schagger, H. (2006). **Nat Protoc** 1, 418-28.
[54] Houstek, J., Andersson, U., Tvrdik, P., Nedergaard, J. and Cannon, B. (1995). **J Biol Chem** 270, 7689-94.
[55] Dubot, A. et al. (2004). **Biochem Biophys Res Commun** 313, 687-93.
[56] Makinen, M.W. and Lee, C.P. (1968). **Arch Biochem Biophys** 126, 75-82.
[57] Fischer, J.C., Ruitenbeek, W., Trijbels, J.M., Veerkamp, J.H., Stadhouders, A.M., Sengers, R.C. and Janssen, A.J. (1986). **Clin Chim Acta** 155, 263-73.
[58] Chowdhury, S.K., Drahota, Z., Floryk, D., Calda, P. and Houstek, J. (2000). **Clin Chim Acta** 298, 157-73.
[59] Rustin, P., Chretien, D., Bourgeron, T., Gerard, B., Rotig, A., Saudubray, J.M. and Munnich, A. (1994). **Clin Chim Acta** 228, 35-51.
[60] Lowry, O.H., Rosebrough, N.J., Farr, A.L. and Randall, R.J. (1951). **J Biol Chem** 193, 265-75.
[61] Baracca, A., Amler, E., Solaini, G., Parenti Castelli, G., Lenaz, G. and Houstek, J. (1989). **Biochim Biophys Acta** 976, 77-84.
[62] Pecina, P. et al. (2003). **Biochim Biophys Acta** 1639, 53-63.
[63] Kunz, W.S. et al. (1993). **Biochim Biophys Acta** 1144, 46-53.
[64] Wenchich, L., Drahota, Z., Honzik, T., Hansikova, H., Tesarova, M., Zeman, J. and Houstek, J. (2003). **Physiol Res** 52, 781-8.
[65] Pecina, P., Gnaiger, E., Zeman, J., Pronicka, E. and Houstek, J. (2004). **Am J Physiol Cell Physiol** 287, C1384-8.
[66] Floryk, D. and Houstek, J. (1999). **Biosci Rep** 19, 27-34.
[67] Wanders, R.J., Ruiter, J.P., Wijburg, F.A., Zeman, J., Klement, P. and Houstek, J. (1996). **J Inherit Metab Dis** 19, 133-6.
[68] Ouhabi, R., Boue-Grabot, M. and Mazat, J.P. (1998). **Anal Biochem** 263, 169-75.
[69] Chomyn, A. (1996). **Methods Enzymol** 264, 197-211.
[70] Chrzanowska-Lightowlers, Z.M., Temperley, R.J., Smith, P.M., Seneca, S.H. and Lightowlers, R.N. (2004). **Biochem J** 377, 725-31.
[71] Brantova, O., Tesarova, M., Hansikova, H., Elleder, M., Zeman, J. and Sladkova, J. (2006). **Ultrastruct Pathol** 30, 239-45.
[72] Sambrook, J. and Russell, D.W. (2001) Molecular cloning: A Laboratory Manual*,* 3rd edn., Cold Spring Harbor Laboratory Press. NY.

8 LIST OF ORIGINAL ARTICLES

Publications *in extenso*, which are a base for this PhD thesis

Fornuskova D, Stiburek L, Wenchich L, Vinsova K, Hansikova H, Zeman J. **2010**. Novel insights into the assembly and function of human nuclear-encoded cytochrome c oxidase subunits 4, 5a, 6a, 7a and 7b. **Biochem J** 428(3):363-74. ***IF 5.155***

Stiburek L, **Fornuskova D**, Wenchich L, Pejznochova M, Hansikova H, Zeman J. **2007**. Knockdown of human Oxa11 impairs the biogenesis of F1Fo-ATP synthase and NADH:ubiquinone oxidoreductase. **J Mol Biol** 374(2):506-16. ***IF 4.472***

Fornuskova D, Brantova O, Tesarova M, Stiburek L, Honzik T, Wenchich L, Tietzeova E, Hansikova H, Zeman J. **2008**. The impact of mitochondrial tRNA mutations on the amount of ATP synthase differs in the brain compared to other tissues. **Biochim Biophys Acta** 1782(5):317-25. ***IF 4.579***

Jesina P, Tesarova M, **Fornuskova D**, Vojtiskova A, Pecina P, Kaplanova V, Hansikova H, Zeman J, Houstek J. **2004**. Diminished synthesis of subunit a (ATP6) and altered function of ATP synthase and cytochrome c oxidase due to the mtDNA 2 bp microdeletion of TA at positions 9205 and 9206. **Biochem J** 383(Pt. 3):561-71. ***IF 4.278***

Vojtiskova A, Jesina P, Kalous M, Kaplanova V, Houstek J, Tesarova M, **Fornuskova D**, Zeman J, Dubot A, Godinot C. **2004**. Mitochondrial membrane potential and ATP production in primary disorders of ATP synthase. **Toxicol Mech Methods** 14(1-2):7-11. ***IF 0.464***

Stiburek L, Kostkova O, **Fornuskova D**, Tesarova J, Wenchich L, Houstek J, Zeman J. **2010**. The mitochondrial ATP-dependent protease YME1L controls the deleterious accumulation of non-assembled OXPHOS subunits. *Submitted for publication to* Mol Cell Biol. *IF 6.057*